JACS
JOURNAL OF THE AMERICAN CHEMICAL SOCIETY

Communication

pubs.acs.org/JACS

Surface-Induced Conformational Changes in Doped Bovine Serum Albumin Self-Assembled Monolayers

Edith Beilis,[†,‡] Bogdan Belgorodsky,[‡] Ludmila Fadeev,[‡] Hagai Cohen,[∥] and Shachar Richter[†,§,*]

[†]University Center for Nanoscience and Nanotechnology, [‡]School of Chemistry, Raymond and Beverly Sackler Faculty of Exact Sciences, and [§]Department of Materials Science and Engineering, Tel Aviv University, Tel-Aviv, Israel 6997801

[∥]Department of Chemical Research Support, Weitzman Institute of Science, Rehovot, Israel 7610001

Supporting Information

ABSTRACT: Evidence for considerable stabilization of doped bovine serum albumin (BSA) molecules upon adsorption on gold surfaces is provided. This is compared to the surface-induced conformational changes of the bare BSA and its corresponding monolayer. The BSA unfolding phenomenon is correlated with dehydration, which in turn enables improved monolayer coverage. The stabilization mechanism is found to be partially controllable via nanodoping of the BSA molecules, upon which the dehydration process is suppressed and molecular rigidity can be varied. Our experimental data and calculations further point to the intermixing of structural characteristics and inherent molecular properties in studies of biological monolayers.

Self-assembly of biomolecules from solution onto solid surfaces is a common technique used in bioelectronics.[1,2] In this method, the molecules are introduced to the surface from solution, thus their conformation in the aqueous medium, which is mediated by intramolecular forces and surrounding intermolecular hydrogen bonds, can be significantly altered upon adsorption.[3] This process should in turn affect the properties of the resulting bio self-assembled monolayer (SAM) by means of its surface coverage and average thickness as well as its electrical and optical properties. In recent studies, controlled changes in electronic and optical properties of protein-based SAMs were achieved by means of doping (hosting foreign species).[4−6] Nevertheless, in all of these studies the conformational effect upon adsorption as a result of doping is still unprecedented. Here we show how, by doping bovine serum albumin (BSA) protein with tetraphenyl-21H,23H-porphine (TPP) and its metallo-derivatives with copper and iron (Figure 1), prior to adsorption, one can stabilize the BSA structure and thus affect the surface-induced conformational changes (secondary structure) upon adsorption. We further point on the correlation between the structure of the adsorbed protein and the morphological properties of the SAM.

TPP and its derivatives are distinguished by their synthetic versatility, thermal stability, enhanced π-electron system and unique opto-electrical properties. The difference in the porphyrin's properties such as electronic structures and optical spectra may be related to the metal atoms incorporated in the center of the porphyrin molecule.[7] Thus, they can be utilized as optically and electrically effective dopants of the protein, which is known for its extraordinary ability to reversibly bind small and mainly hydrophobic molecules. Doped BSA complexes were prepared by adding TPP derivatives [15 mM stock solutions in dimethyl sulfoxide, (DMSO)] to BSA [30uM stock solution in aqueous phosphate buffer, pH 7.2 10Mm], at a fixed molar ratio of 5:1. Following incubation, the complexed solutions were separated and purified with the use of a Sephadex G-25 gel-permeation column (Pharmacia Biotech) with phosphate buffer (10 mM, pH 7.2).

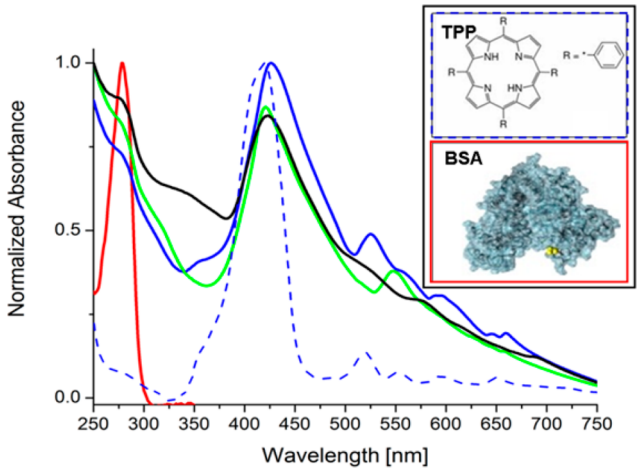

Figure 1. Normalized UV−vis absorption spectra of solutions of BSA (red), TPP (dashed blue), doped BSA with TPP (blue), TPPCu (green), and TPPFeCl (black). Inset: schematic illustration of molecular structures of TPP (top) and calculated BSA N-form structure (yellow, the free cysteine residue on the protein surface (Cys-34)).

The complexation of BSA-TPP derivatives was assessed by means of UV−vis absorption spectroscopy (Figure 1). Doped BSA spectra consist of a peak in the UV region attributed to the aromatic residues of BSA (λ_{max} = 280 nm) and two additional bands in the visible region: Soret (400−500 nm) and Q (500−700 nm) attributed to the TPP derivatives. The spectra reveal distinct "fingerprints" of the complexes (mainly in the Q-band), indicating the formation of distinguishable complexes.[8] The binding of TPP and its derivatives to BSA is attributed to the

Received: October 24, 2013
Published: April 14, 2014

   dx.doi.org/10.1021/ja410754t | J. Am. Chem. Soc. 2014, 136, 6151−6154

ligand's high affinity for BSA binding sites, mainly in the subdomains IIA, IA, and IB[9] which contain the hydrophobic fluorophores tyrosine and tryptophan (see simulations in the Supporting Information, SI). Therefore, steady-state fluorescence spectroscopy can be used to monitor the complexation of BSA-TPP derivatives (Figure 2), by means of the optical

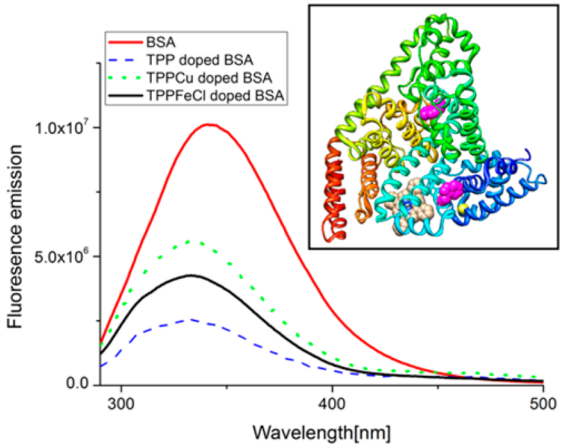

Figure 2. Steady-state fluorescence spectra (λ_{ex} = 280 nm) indicating a blue shift in emission maximum, from 343 nm (undoped BSA) to ~332 nm (doped BSA). Inset: the proposed TPP binding site as obtained by patchdock simulation. The Trp135 and Trp214 residues are highlighted in pink and the Cys34 site in yellow.

overlap between the BSA hydrophobic fluorophore emission and the TPP chromophore absorption. Figure 2 clearly shows quenching of the BSA fluorescence in the presence of TPP derivatives, accompanied by a blue shift of the maximum emission wavelength. As previously shown[10] these observations indicate strong hydrophobic interactions and energy transfer between BSA hydrophobic moieties and the TPP derivatives. Yet, the exact binding location of TPP derivatives in BSA is an open question, since no *a priori* data indicating a feasible TPP binding site are known. We complementarily approximated the TPP binding site by means of docking studies[11] (see also SI). Figure 2 (inset) shows the result of high-score calculations which suggest a possible TPP binding site at subdomain IB within the BSA host molecule. This result supports those of previous studies of complexation of other proteins.[12]

Next, we examined the effect of doping on the properties of the SAM. Monolayers of undoped BSA and metallo-TPP-doped BSA complexes were prepared by immersing samples of annealed hydrophilic gold surfaces in freshly prepared solutions (for details see SI). It has been shown that, as protein molecules adsorb on solid surfaces, they may undergo surface-induced structural transformations (mainly unfolding)[13] which could be monitored by means of IR measurements.[14] Here, we used the surface-sensitive polarization modulation infra-red reflectance absorption spectroscopy (PMIRRAS) to assess the conformational state (manifested as secondary-structure percentages) of the adsorbed doped BSA vs that of undoped BSA (see also SI). When IR techniques are used to study surface-adsorbed proteins, the main spectral region of interest includes the Amide-I and -II bands. These bands arise from characteristic vibration modes of the protein backbone (affected by adsorption), typical of all proteins.[15] In this context, the Amide-I represents mainly the C═O stretching vibrations of the amide group, and Amide-II represents mainly in-plane N−H bending and C−N stretching modes. Figure 3 shows spectra of the Amide I and II region. The differences shown in band

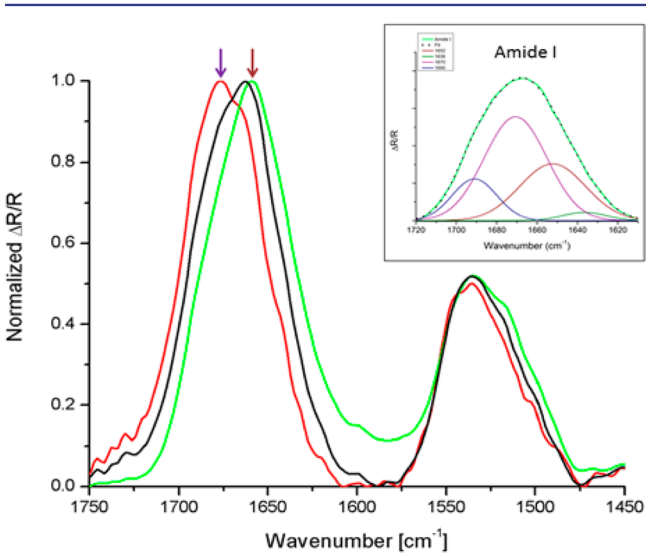

Figure 3. Normalized representative PMIRRAS spectra in the Amide-I (1700−1600 cm^{-1}) and II (1500−1600 cm^{-1}) region of self-assembled BSA monolayers: undoped (red), TPPCu-doped (green), and TPPFeCl-doped (black) . A clear shift of the Amide I maximum is observed upon doping. Inset: A representative example of Amide-I deconvolution procedure (TPPCu-doped BSA). Peaks assignemnt[14,16] at 1636 cm^{-1} (β-sheet/extended chains, dark green), 1652 cm^{-1} (α-helices, deep red), 1670 and 1690 cm^{-1} (β-sheet or β-turn, deep purple and blue).

shapes and the clear shift in band maxima (Figure 3 and Table S6) indicate that undoped and doped proteins exhibit different conformations upon adsorption. For further quantitative analysis of the secondary structure we focus on the Amide-I band. Differences in this band arise from varying secondary structures within the protein backbone which give rise to different vibrational frequencies, expressed by the components obtained from the IR deconvoluted band. Figures 3(inset) and S5 show representative spectra and deconvolution of the Amide I band.[16] We followed the procedure in which the integrated areas of fitted components are normalized to the total Amide-I area and assumed them to be directly proportional to the relative amount of the corresponding secondary structures.[16] Specifically, the peaks were assigned according to their maxima: 1663−1695 cm^{-1} assigned to β-sheet and β-turn structures, 1648−1655 cm^{-1} to α-helices, and 1615−1639 cm^{-1} to extended chains and β-sheets.[13−16] While the BSA conformation in solution [at pH range of 4.5−8 (N-form)[17]] can be characterized by its high α-helical content (roughly 67%), corresponding to a compact form, adsorbed BSA exhibits a major decrease in its α-helical content and a corresponding increment in the more stable, unfolded, β-sheet/turn structures.[13−16] In this respect the effect of doping on these marked changes is an intriguing question.

Figure 4 shows the secondary structure percentages as obtained from the Amide I analysis. Our results clearly indicate that the doping action results in substantial conformational changes upon adsorption. This is expressed by an increasing α-helices content and a corresponding decrease in the content of β-sheet/turn secondary structures, realized at the doped protein monolayers with respect to the undoped ones. Our findings indicate that the undoped BSA molecules are more distorted

dx.doi.org/10.1021/ja410754t | J. Am. Chem. Soc. 2014, 136, 6151−6154

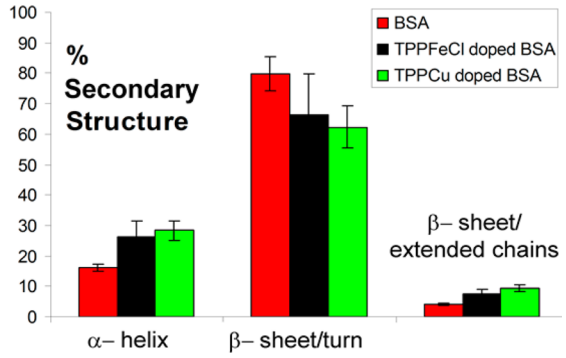

Figure 4. Analysis of secondary structure percentages as extracted from deconvoluted Amide I bands.

upon adsorption, while the doped BSA molecules retain a higher degree of their original structure in solution, expressed by higher α-helical content.

Further insight on this phenomenon is provided by high resolution X-ray photoelectron spectroscopy (XPS, see also SI). Table 1 shows representative atomic concentrations, as measured by XPS, normalized to the nitrogen (N) signal. Significant variations in oxygen (O) content are observed, associated with the amount of tightly bound water molecules within the protein. This finding agrees with previous studies showing protein distortions upon adsorption that is followed by dehydration of the adsorbed BSA.[14] Higher O/N ratios are found for doped BSA, compared to the undoped one, which are related to oxygen originated in the protein and to tightly bound water. Values after subtraction of other O-containing components are given in brackets, Table 1. This suggests that the doped molecules retain, upon adsorption, a higher degree of their original structure (compared to the undoped ones) due to a lower degree of dehydration (for details, quantitative analysis and the XPS angle resolved spectra, see Figure S4 and Table S4). Independently, the density of BSA molecules can be estimated from the relative intensity of the Au signal (see Table S2).

Table 1. Theoretical and XPS-Derived Atomic Concentrations of Various BSA SAMs, Normalized to the Nitrogen Content[a]

	atomic ratio	S/N	O/N	C/N
	theoretical	0.05	1.15	3.76/3.79
undoped BSA	measured	0.07	1.78 (*1.52)	3.66
TPPFeCl-doped BSA	measured	0.12	2.03 (*1.78)	3.73
TPPCu-doped BSA	measured	0.19	2.30 (*1.85)	3.93

[a]Brackets (*): O/N atomic ratio for the overlayer oxygen (interface oxygen subtracted). Note the significant increase of the latter in the doped samples.

An average layer thickness is thus extracted, assuming photoelectron attenuation across an ideal uniform overlayer. Next, to obtain the surface coverage of these molecules, namely the deviations from a uniform film model, we inspect the C, S, and N signals. The C/N ratio is similar in all layers, but the S/N shows significant differences, far beyond the expected dopant-related additions, and the varying S-component is mainly that of reduced S (see Table S3). Thus, our detailed angle-dependent XPS data point to small S-containing moieties that cover the inter-BSA areas, with minimal disturbance as of the BSA arrangement. Importantly, the correlation between Au signal and S/N (Tables S2 and S1, respectively) may suggest that the undoped BSA molecules achieve a more uniform coverage via dehydration and structural reconstruction (also expressed by the lowest O/N ratio) a feature not easily realized by the doped BSA.

Next, we simulate the effect of the adsorbed protein's conformation on the SAMs surface coverage. The simulation is based on the following assumptions: (i) the approximated shape of adsorbed doped BSA is of an equilateral triangle with estimated dimensions of 8 nm (edge length) by 3 nm (thickness),[18] corresponding to the reported dimensions of the pH depended BSA N-form; (ii) the undoped surface-induced modified conformation is represented by an ellipse with a footprint area of 14 nm by 4 nm;[19] and (iii) the BSA adsorbs on the surface in a "side-on" orientation' (as verified by AFM, SI). Our simulations allow the protein molecules to adsorb on the surface at randomly chosen locations and rotation angles. As the protein approaches the surface, an adsorption event takes place only if the selected adsorption site is unoccupied. If an adsorption event fails, a new possible location and rotation angle are randomly chosen. After a predefined number of failed attempts (set at 1000) the simulation is stoped, and surface coverage is calculated.

Figure 5 shows a representative simulation result which clearly supports our experimental findings. Indeed, it is demonstrated that the adsorbed elliptical structures (undoped BSA) exhibit higher surface coverage (46 ± 1%) compared to the equilateral triangles (doped BSA, 42.7 ± 0.5%, calculated from 50 simulations).

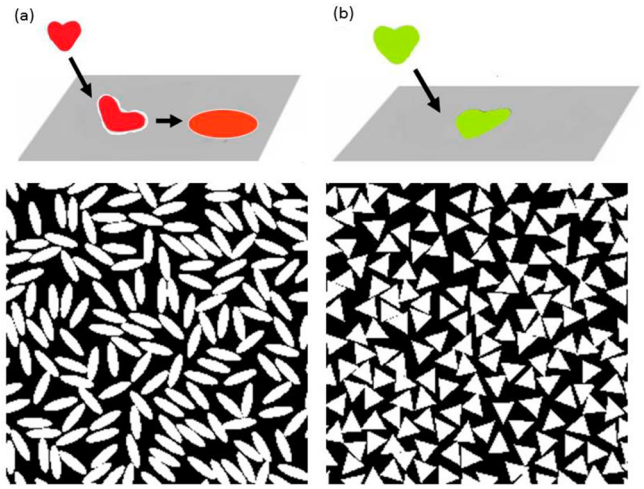

Figure 5. Representative adsorption model results of (a) undoped BSA approximated by an ellipse with a footprint area of 14 × 4 nm and (b) doped BSA approximated by an equilateral triangle with an edge length of 8 nm.

In summary, we explore here the effect of doping of proteins on the resulting SAM. It is shown that doped BSA tends to retain a higher degree of its shape during adsorption, whereas the undoped BSA exhibits conformational flexibility that involves dehydration upon adsorption. Our *ex situ* research may propose interesting implications on *in situ* protein properties and related mechanisms, issues that are not directly addressed here. On the basis of both quantitative analysis of the experimental data and complementing simulations, our data suggest further effects that should not be neglected when the

dx.doi.org/10.1021/ja410754t | J. Am. Chem. Soc. 2014, 136, 6151−6154

physical properties of SAMs, such as electrical and optical characteristics, are explored.

■ ASSOCIATED CONTENT

Supporting Information

Experimental details, AFM images and analysis, additional PMIRRAS and XPS data. This material is available free of charge via the Internet at http://pubs.acs.org.

■ AUTHOR INFORMATION

Corresponding Author

srichter@post.tau.ac.il

Notes

The authors declare no competing financial interest.

■ ACKNOWLEDGMENTS

We would like to thank A. Khatchatouriants, A. Beilis, and M. Gozin for their support. This research was funded by the Tashtiot (no. 0603516842) and the Israel Science Foundation (no. 434/12) funds.

■ REFERENCES

(1) Mentovich, E.; Belgorodsky, B.; Gozin, M.; Richter, S.; Cohen, H. *J. Am. Chem. Soc.* **2012**, *134*, 8468.
(2) Ron, I.; Sepunaru, L.; Itzhakov, S.; Belenkova, T.; Friedman, N.; Pecht, I.; Sheves, M.; Cahen, D. *J. Am. Chem. Soc.* **2010**, *132*, 4131.
(3) Mrksich, M.; Whitesides, G. M. *Annu. Rev. Biophys. Biomol. Struct.* **1996**, *25*, 55.
(4) Hendler, N.; Belgorodsky, B.; Mentovich, E. D.; Richter, S.; Fadeev, L.; Gozin, M. *Adv. Funct. Mater.* **2012**, *22*, 3765.
(5) Della Pia, E. A.; Chi, Q. J.; Elliott, M.; Macdonald, J. E.; Ulstrup, J.; Jones, D. D. *Chem. Commun.* **2012**, *48*, 10624.
(6) Amdursky, N.; Pecht, I.; Sheves, M.; Cahen, D. *J. Am. Chem. Soc.* **2012**, *134*, 18221.
(7) El-Nahass, M. M.; El-Deeb, A. F.; Metwally, H. S.; Hassanien, A. M. *Eur. Phys. J.: Appl. Phys.* **2010**, *52*, 10502.
(8) El-Nahass, M. M.; M. Z, H.; Aziz, M. S.; Makhlouf, M. M. *Spectrochim. Acta, Part A* **2005**, *61*, 3026.
(9) Sulkowska, A.; Maciazek-Jurczyk, M.; Bojko, B.; Rownicka, J.; Zubik-Skupien, I.; Temba, E.; Pentak, D.; Sulkowski, W. W. *J. Mol. Struct.* **2008**, *881*, 97.
(10) Tian, J. N.; Liu, X. H.; Zhao, Y. C.; Zhao, S. L. *Luminescence* **2007**, *22*, 446.
(11) Schneidman-Duhovny, D.; Inbar, Y.; Nussinov, R.; Wolfson, H. J. *Nucleic Acids Res.* **2005**, *33*, W363.
(12) Komatsu, T.; Nakagawa, A.; Curry, S.; Tsuchida, E.; Murata, K.; Nakamura, N.; Ohno, H. *Org. Biomol. Chem.* **2009**, *7*, 3836.
(13) Gray, J. J. *Curr. Opin. Struct. Biol.* **2004**, *14*, 110.
(14) Roach, P.; Farrar, D.; Perry, C. C. *J. Am. Chem. Soc.* **2005**, *127*, 8168.
(15) Kong, J.; Yu, S. *Acta Biochim. Biophys. Sin.* **2007**, *39*, 549.
(16) Desroches, M. J.; Chaudhary, N.; Omanovic, S. *Biomacromolecules* **2007**, *8*, 2836.
(17) Tsai, D. H.; DelRio, F.; Keene, A.; Tyner, K.; MacCuspie, R.; Cho, T. J.; Zachariah, M.; Hackley, V. *Abstr. Pap. Am. Chem. Soc.* **2011**, 242.
(18) Lee, C. T.; Smith, K. A.; Hatton, T. A. *Biochemistry* **2005**, *44*, 524.
(19) Tencer, M.; Charbonneau, R.; Lahoud, N.; Berini, P. *Appl. Surf. Sci.* **2007**, *253*, 9209.